

The Folding Pathway of the Genomic Hepatitis Delta Virus Ribozyme is Dominated by Slow Folding of the Pseudoknots

Durga M. Chadalavada, Susan E. Senchak and Philip C. Bevilacqua*

Department of Chemistry, The Pennsylvania State University University Park, Pennsylvania PA 16802, USA

Hepatitis delta virus (HDV) replicates by a double rolling-circle mechanism that requires self-cleavage by closely related genomic and antigenomic versions of a ribozyme. We have previously shown that the uncleaved genomic ribozyme is subject to a variety of alternative (Alt) pairings. Sequence upstream of the ribozyme can regulate self-cleavage activity by formation of an Alt 1 ribozyme-containing structure that severely inhibits self-cleavage, or a P(-1) self-structure that permits rapid self-cleavage. Here, we test three other alternative pairings: Alt P1, Alt 2, and Alt 3. Alt P1 and Alt 3 contain primarily ribozyme-ribozyme interactions, while Alt 2 involves ribozyme-flanking sequence interaction. A number of single and double mutant ribozymes were prepared to increase or decrease the stability of the alternative pairings, and rates of self-cleavage were determined. Results of these experiments were consistent with the existence of the proposed alternative pairings and their ability to inhibit the overall rate of native ribozyme folding. Local misfolds are treated as internal equilibrium constants in a binding polynomial that modulates the intrinsic rate of cleavage. This model of equilibrium effects of misfolds should be general and apply to other ribozymes. All of the alternative pairings sequester a pseudoknot-forming strand. Folding of ribozymes containing Alt P1 and Alt 2 was accelerated by urea as long as the native ribozyme fold was sufficiently stable, while folding of mutants in which both of these alternative pairings had been removed were not stimulated by urea. This behavior suggests that the pseudoknots form by capture of an unfolded or appropriately rearranged alternative pairing by its complementary native strand. Fast-folding mutants were prepared by either weakening alternative pairings or by strengthening native pairings. A kinetic model was developed that accommodates these features and explains the position of the rate-limiting step for the G11C mutant. Implications of these results for structural and dynamic studies of the uncleaved HDV ribozyme are discussed.

© 2002 Elsevier Science Ltd.

Keywords: RNA folding; kinetic trap; viral replication; PKR; conformational change

*Corresponding author

Abbreviations used: A/B, an RNA with a 5'-end of A and a 3'-end of B; Alt X₃, the 3'-strand of the pairing Alt X; AS, antisense oligomers; AS(-30/-7), antisense DNA oligomer complementary to HDV nucleotides -30 to -7; AS(-30/-3), antisense DNA oligomer complementary to HDV nucleotides -30 to -3; Hepes, 4-(2-hydroxyethyl)-1-piperazineethanesulfonic acid; HDV, hepatitis delta virus; Mes, [2-(N-morpholino)ethanesulfonic acid]; N, native ribozyme conformation; P, product or self-cleaved ribozyme.

E-mail address of the corresponding author: pcb@chem.psu.edu

Introduction

Ribonucleic acids can fold into a diverse set of structures with various functions, including catalysis.¹ Structures of numerous RNA molecules and RNA-protein complexes have been solved; recent examples include the hairpin ribozyme² and structures of the 50 S and 70 S ribosomes.^{3,4} These structures and their associated functions arise from complex folding and assembly pathways. The folding pathway of a number of RNA and RNP complexes have been investigated mechanistically,

including tRNA, the Tetrahymena ribozyme, the RNase P ribozyme, the assembly of the b15 group I intron with the CBP2 protein, and the assembly of the ribosome.^{5–11} These studies have indicated that large RNAs generally fold slowly, on the minutes or longer timescale. Slow folding has been attributed to the formation of misfolded RNAs with long lifetimes, referred to as kinetic traps.¹² In many of these cases, it appears that non-native secondary structures form that are slow to dissociate.

Recently, a number of fast-folding ribozymes that avoid kinetic traps have been engineered.^{6,9,10,13–18} Approaches to making fast folders include site-directed mutagenesis, *in vitro* selection, and circular permutation. The bases for fast-folding RNAs include strengthened native pairings,¹⁴ prevention of premature formation of native secondary structure,⁶ and pre-assembly of native secondary structure in collapsed intermediates.¹⁰ Fast-folding RNAs provide useful experimental tools, since they allow focus on issues other than unfolding of alternative pairings, including tertiary structure formation, metal ion binding, protein binding and RNA catalysis.

Folding of large RNAs has been described as a hierarchical process in which individual subdomains fold independently prior to higher-order structure formation.¹⁹ For example, the 160 nt P4-P6 domain from Tetrahymena folds rapidly and independently of the rest of the ≈ 400 nt ribozyme.^{7,15} In nucleic acids, local hydrogen bonding and stacking interactions are strong and, in many instances, this has allowed results from model systems to be applied to larger systems. For example, thermodynamic rules elucidated from model duplexes and hairpins have been used to predict the secondary structure of large RNAs.²⁰ RNA folding studies on smaller ribozymes have also revealed complex RNA folding events, including tertiary folding of the hairpin, hammerhead, and VS ribozymes.^{21–24} Also, early studies on tRNA indicated that under certain conditions, RNA tertiary structure can form in several milliseconds from a pre-formed secondary structure.⁵ Studies on small pseudoknot-containing RNAs, such as the hepatitis delta virus (HDV) ribozyme, may also provide insight into fundamental RNA folding processes.

HDV contains an ≈ 85 nt ribozyme that is found in closely related genomic and antigenomic forms.²⁵ The crystal structure of the self-cleaved form of the genomic ribozyme is available at 2.3 Å resolution, and reveals a structure containing two nested pseudoknots.²⁶ The HDV ribozyme undergoes rapid cleavage under certain conditions allowing the fractional occupancy of the native state to be probed. Thus the HDV ribozyme provides a good model system in which to study complex RNA folding events.

HDV is a human pathogen that enhances the virulence of hepatitis B virus infections.^{27–29} The genome has a circular RNA of ≈ 1700 nucleotides and forms a highly base-paired, rod-like structure.

HDV replicates by a double rolling-circle model and the nascent RNA is processed into monomers by self-cleavage of the genomic or antigenomic ribozyme. The linearized monomers appear to be ligated by a host factor to form the circular genome again.³⁰ After ligation, the ribozyme must be kept inactive, and this is achieved by base-pairing to a downstream stretch of nucleotides termed the attenuator. A detailed understanding of the folding pathway of this ribozyme may therefore provide insight into replication of HDV and help identify targets for therapeutics. A thorough understanding of HDV folds and conformational changes may also reveal the basis behind reports that HDV can both activate and inhibit the antiviral protein, PKR.³¹

Prior studies from our laboratory revealed that the pre-cleaved genomic ribozyme can exist in a non-native secondary structure that contains several alternative pairings.³² These include alternative pairings between ribozyme and upstream flanking sequence, Alt 1 and Alt 2, and an alternative pairing within the ribozyme itself, Alt 3. We provided evidence that sufficiently long upstream flanking sequence (–54) can form a self-structure, P(–1), that sequesters an upstream inhibitory stretch in Alt 1 *in cis* and leads to rapid formation of native structure and co-transcriptional cleavage.³² In addition, the inhibitory stretch can be sequestered *in trans* by addition of antisense (AS) oligomers resulting in a rate identical with that of the reaction *in cis*.³² Addition of AS oligomers releases the very 3'-end of the ribozyme from Alt 1, and in this way may mimic some of the folding events that occur co-transcriptionally.³²

Here, we test the effect of the Alt 2 and Alt 3 pairings on the folding of the ribozyme. In addition, the effect of an alternative pairing of P1, designated Alt P1, on the folding of the ribozyme was tested. We made a series of single and double mutants that increased or decreased the stability of alternative and native pairings, and examined their effects on the ability of the ribozyme to attain the native pairing. The results of these studies revealed several fast-folding HDV genomic ribozymes, and were used to develop an initial kinetic model for folding of the ribozyme.

Results

Identification of intermediates in folding

We examined the predicted folds for RNA sequences containing upstream nucleotides and the 5'-portion of the wild-type HDV ribozyme by free energy minimization using *mfold* 3.1.^{20,33} In its native fold, the 5'-portion of the ribozyme interacts with the very 3'-portion to form the pseudoknot pairing, P2 (Figure 1).²⁶ We suspected that the 5'-strand of P2 might be susceptible to alternative local folds that would compete with pseudoknot folding. Computer folding of a –8 to 44 fragment of the RNA revealed two folds that were signifi-

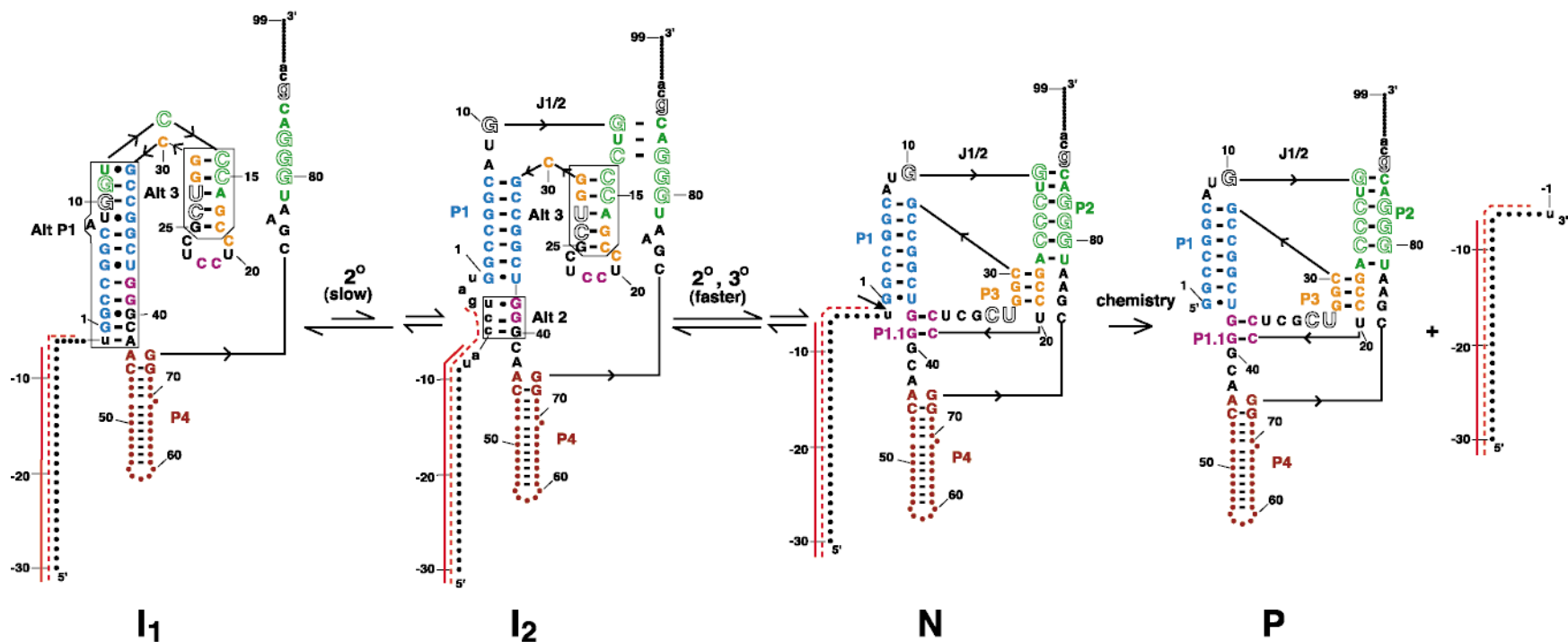


Figure 1. Secondary structure of intermediates I_1 and I_2 , the native fold, N , and the cleaved product form, P . The structure is color-coded based on the native fold. Pairings in N are assumed to be the same as in P , based on results from extensive mutagenesis experiments on the pre-cleaved form of the ribozyme being consistent with the crystal structure of the cleaved form of the ribozyme (results here and elsewhere).^{25,26,41} Secondary structures of I_1 and I_2 are based on structure mapping³² and the mutants tested in this study. Pairings are oriented on the page in a native-like fashion for convenience only; their actual juxtaposition is unknown. Only the native fold can lead to product, P . The ribozyme sequence is shown in upper case and the flanking sequence in lower case. Part of $P4$ and the upstream sequence are represented as dots for simplification. Negative values are used for nucleotides upstream of the cleavage site, indicated by an arrow. J1/2 is the joining region between P1 and P2 consisting of A8, U9, and, depending on the mutant, G10. Individual mutations made in this study are shown in larger, outlined font. Alternative pairings in I_1 and I_2 are boxed and denoted Alt 2, Alt 3, and Alt P1. The GG single mismatch is depicted with a dot, since a GG mismatch with the closing base-pairs shown has a ΔG_{37}° of -2.6 kcal/mol.³⁵ Red lines represent binding sites of antisense oligomers that break the inhibitory Alt 1 pairing.³² The continuous line denotes AS(-30/-7), and the broken line denotes AS(-30/-3). Equilibria favor I_1 over I_2 ; sequential arrows depict possible intermediates. Slow and fast are based on rates with mutants that occupy these states, and possible secondary and tertiary rearrangements are indicated.

cantly different. (We chose to fold this fragment, since it is unlikely to interact with the stable and well-determined P4 hairpin that bounds it on the 3'-end; identical structures were identified when the entire ribozyme sequence was folded.) The structure identified with the lowest ΔG_{37}° , I_1 , contained two alternative pairings, Alt P1 and Alt 3 (Figure 1). The next significantly different suboptimal structure, I_2 , was predicted to be 4.1 kcal/mol (1 cal = 4.184 J) less stable in ΔG_{37}° and contained two alternative pairings, Alt 2 and Alt 3 (Figure 1). Alt P1 and Alt 2 are mutually exclusive, and formation of Alt 2 is compatible with formation of a native P1.

The three alternative pairings in I_1 and I_2 were tested by examining rates for self-cleavage by 18 mutants using two antisense oligomers. The Alt P1 and Alt 3 pairings involve ribozyme-ribozyme interactions and so were tested by ribozyme mutations that affected the stability of the alternative pairings, typically in the background of either unperturbed or restored native pairings. The Alt 2 pairing involves ribozyme-flanking sequence interactions and was tested using lengthened antisense oligomers that have the potential to disrupt Alt 2. Observed rate constants for cleavage should be related to the fraction of the ribozyme in the native fold, since care was taken to maintain or restore

the native secondary and tertiary structures of the mutant ribozymes, and because the intrinsic rate of cleavage is rapid. A more extensive consideration of the relationship between observed rate constants and ribozyme misfolding is presented in the Discussion.

Testing the Alt P1 helix with RNA mutations

The kinetic profile for self-cleavage of the wild-type RNA in the presence of AS(-30/-7) was biphasic, with $\approx 30\%$ of the reaction proceeding in a burst phase (Table 1, Figure 2(a)). The burst phase was complete in 15 seconds, requiring a rapid-mixing technique to obtain a good kinetic profile. Using a rapid-quench apparatus for the fast time-points, we determined the rate constants for the burst and slow phases to be 12 and 0.17 min^{-1} , respectively (Table 1). A burst amplitude of 30% was obtained by both hand-mixing and rapid-quench techniques. This fast-reacting fraction may represent a population of the RNA molecules that can more readily adopt the native conformation and cleave. The slow-reacting fraction may represent a population that is trapped in stable non-native pairings that have to rearrange before the ribozyme can achieve the catalytically active fold. Alt P1 is a non-native pairing predicted

Table 1. Effect of mutants on the rate of self-cleavage in the presence of 10 μM AS (-30/ -7)

RNA	k_{obs} (min^{-1}) ^a	Burst/complete ^a (%/%)	Fold effect ^b	Basis ^c
wt (slow phase)	0.17 ± 0.01		1	Start from I_1
wt (burst phase) ^d	12.0 ± 0.9	30/90	70.6	Start from I_2
<i>A. Mutants of Alt P1</i>				
G10A	5.8 ± 1.1		34	Destabilize Alt P1
G11C ^d	7.1 ± 0.7		42	Destabilize Alt P1
<i>B. Mutants of Alt 3/P2</i>				
C13G	0.00006 ^e		0.00035	Stabilize Alt 3/destabilize P2
C13A	0.019 ± 0.006		0.1	Destabilize P2
G82U	0.042 ± 0.01		0.25	Destabilize P2
C13A:G82U	0.07 ± 0.01	27/95	0.4	Restore P2
C14G	0.15 ± 0.04	40/90	1	Destabilize Alt 3 and P2
G81C	0.06 ± 0.016		0.35	Destabilize P2
C14G:G81C	cotxn ^f		Large ^g	Destabilize Alt 3/restore P2
C15A	2.2 ± 0.17		13	Lg. Destabilization of Alt 3/destabilize P2
G80U	0.1 ± 0.04	35/90	0.59	Destabilize P2
C15A:G80U	cotxn ^f		Large ^g	Lg. Destabilization of Alt 3/restore P2
U27A	cotxn ^f		Large ^g	Lg. Destabilization of Alt 3
U27 Δ ^h	cotxn ^f		Large ^g	Lg. Destabilization of Alt 3
C26 Δ	cotxn ^f		Large ^g	Lg. Destabilization of Alt 3
G85C	2.2 ± 0.5		13	Stabilize P2

^a Data were fit to equation (1). k_{obs} is for the slow phase, unless otherwise noted, and % burst and % complete were determined as described in Materials and Methods. Burst phase is reported only for reactions that were biphasic. Unless otherwise noted, the percentage complete was between 80 and 95. Errors shown are standard deviations of three or more experiments.

^b Fold-effect are for k_{obs} relative to the wild-type RNA slow phase.

^c Basis gives the structural basis for the fold-effect based on our best model for the data.

^d Determined by rapid-quench.

^e Reaction was not complete after 24 hours. These data were well fit by the linear approximation, $f_{\text{cleaved}} = k_{\text{obs}} t$.

^f Self-cleavage was rapid, and extensive during transcription.

^g Not quantified, but a large effect.

^h Also, uncleaned U27 Δ was prepared by transcription at 30°C and used in rapid-quench self-cleavage assays. A burst phase of 39 min^{-1} (40%) was observed, consistent with rapid cleavage of the Alt 3-destabilizing class of mutants.

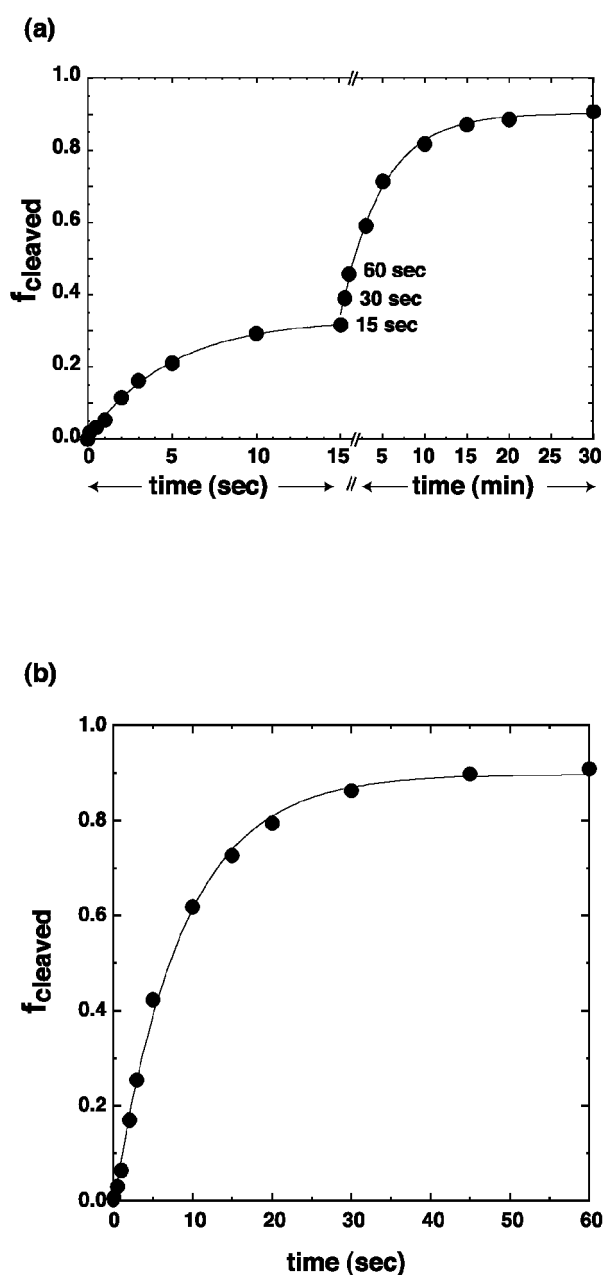


Figure 2. Kinetic traces for the self-cleavage reactions of wild-type and G11C ribozymes in the presence of AS(-30/-7). The data are a combination of values obtained by hand-mixing and rapid quench. (a) Kinetic trace for wild-type ribozyme. The first transient was essentially complete before the start of the second, so equation (1) was used to fit each transient separately; similar rates were obtained with a double-exponential equation. Constants for the burst phase, obtained by rapid mixing, were $A = 0.33$, $B = -0.33$, and $k_{\text{obs}} = 12 \text{ min}^{-1}$. Constants for the slow phase, obtained by hand-mixing, were $A = 0.90$, $B = -0.56$, and $k_{\text{obs}} = 0.17 \text{ min}^{-1}$. The x -axis is broken to accommodate fast and slow phases. Time-points at the intersection of the phases are labeled on the plot. (b) Kinetic trace for G11C ribozyme. Time-points to 20 seconds were obtained by rapid mixing and the remainder by hand-mixing. Constants were $A = 0.89$, $B = -0.91$, and $k_{\text{obs}} = 6.6 \text{ min}^{-1}$.

to be present only in intermediate I_1 , which involves ribozyme-ribozyme interactions and disrupts native P1, P2 and P1.1 helices (Figure 1). If the Alt P1 pairing in I_1 were responsible for at least a portion of the reduced catalytic activity of the wild-type ribozyme, then disrupting this interaction might allow the slow-reacting fraction of the ribozyme to cleave faster.

In an attempt to disrupt the Alt P1 pairing, single mutations were introduced at positions 10 and 11 of the ribozyme. These mutations were designed to weaken Alt P1 without compromising the stability of the native fold (Figure 1). (The G11C ribozyme was expected to form a modified P2 pairing with a bulged C84 followed by CG, GC, and UA base-pairs, while the G10A ribozyme should retain the same 6 bp P2 helix as the wild-type.) Computer predictions by *mfold* 3.1 on G10A and G11C -8/44 fragments supported these ideas, as I_2 was now predicted to be slightly more stable than I_1 . Both G10A and G11C mutant RNAs exhibited monophasic kinetics (Figure 2(b) and data not shown) with similar rate constants of 5.8 and 7.1 min^{-1} for self-cleavage in the presence of AS (-30/-7) (Table 1). Lack of a slow phase for these mutants supports the model in which Alt P1 represents a significant barrier to reaction of I_1 , and suggests Alt P1 has been largely removed in G10A and G11C. In addition, cleavage rates for G10A and G11C were similar (only about twofold slower) to the cleavage rate for the burst phase reaction of the wild-type. This suggests that the wild-type ribozyme may partition between I_1 and I_2 , and that G10A and G11C originate from I_2 . Experiments with different length AS oligomers and urea also support this idea (see below).

Testing the Alt 2 helix with antisense oligomer AS(-30/-3)

The native P1 pairing in intermediate I_2 was predicted to be associated with a short alternative pairing, Alt 2 (Figure 1). The Alt 2 pairing involves interactions between upstream-flanking nucleotides and three essential guanine bases in the ribozyme, G38-G40, potentially sequestering P1.1₃. The Alt 2 pairing was tested by initiating reactions with the lengthened antisense oligomer AS(-30/-3), which was predicted to release the P1.1-forming bases from Alt 2 (Figure 1). This approach was chosen over mutation of the three Gs, since these residues and/or their pairing partners are conserved and essential for secondary and tertiary interactions in the native fold.²⁶ According to this model, only mutant RNAs with Alt 2, present in I_2 , would be enhanced by AS(-30/-3), while RNAs primarily in I_1 would not be enhanced by AS(-30/-3) (see Figure 1). To test this idea, cleavage kinetics for various mutant RNAs were compared in the presence of AS(-30/-3) and AS(-30/-7) (Table 2). (Results described in this section refer to the 0 M urea data of Table 2.)

Table 2. Effect of urea and antisense oligomers on the rate of self-cleavage

RNA	[Urea]			
	0 M	2 M	4 M	6 M
A. AS (-30/-7)^a				
wt (slow phase)	0.17 ± 0.01	0.082 ± 0.007	0.067 ± 0.01	0.043 ± 0.004
wt (burst phase) ^b	12.0 ± 0.9 (30/90)	24.0 ± 1.1 (40/90)	21.6	15.6
G11C ^b	7.1 ± 0.7	22.9 ± 1.2	25.8 ± 1.3	18.9
C14G	0.15 (40/90)	0.47 (18/90)	0.38 (monophasic)	0.07 (monophasic)
C15A	2.2	2.5	0.54	0.04
G85C	2.2	5.6	4.4	5.3
C14G:G85C	0.73	2.9	2.1	0.28
C15A:G85C	2.5	5.5	2.9	0.38
B. AS (-30/-3)^a				
wt (slow phase)	0.092 ± 0.007	0.095 ± 0.002	0.066 ± 0.004	0.041 ± 0.003
wt (burst phase) ^b	23.8 ± 1.4 (30/90)	24.4 ± 1.7 (43/90)	22.2	16.2
G11C ^b	29.3 ± 0.9	25.2 ± 2.2	19.3 ± 1.9	15.6
C14G	0.15 (40/90)	0.45 (20/90)	0.37 (monophasic)	0.07 (monophasic)
C15A	3.1	2.2	0.57	0.07
G85C	6.5	12.0	11.7	7.2
C14G:G85C	2.6	5.1	2.8	0.42
C15A:G85C	3.4	5.3	3.3	0.26

Data were fit to equation (1). k_{obs} values are in units of min^{-1} , and are provided for the slow phase unless otherwise noted. The % burst and % complete are given in parentheses. Unless otherwise noted, the percentage complete was between 80 and 95. Errors shown are standard deviations of three or more experiments. Values without error bars are the average of two experiments.

^a AS (-30/-7) and AS (-30/-3) are present at 10 μM .

^b Determined by rapid-quench.

The C14G and C15A mutants changed residues only in Alt 3. Since the I_1/I_2 equilibrium does not appear to involve changes in Alt 3, C14G and C15A were not expected to break Alt P1 and form Alt 2 (Figure 1), although they do appear to break Alt 3 (see the next section). Consistent with this model, the cleavage activities of C14G (slow phase) and C15A were not significantly affected by lengthening the AS oligomer (Table 2). In contrast, G11C revealed a fourfold faster rate in the presence of AS(-30/-3) than AS(-30/-7), suggesting a preference for a native P1 and a concomitant Alt 2 pairing that interferes with folding (Table 2 and Figure 3(a)). Qualitatively similar results were obtained for G10A by hand-mixing (data not shown). These data suggest that folding of G10A and G11C originates from the I_2 intermediate, consistent with results from the previous section.

Reactions carried out on G85C revealed an approximate threefold rate increase in the presence of the lengthened AS oligomer, suggesting G85C at least partially occupies I_2 (Table 2). However, it appears that this rate increase has a different mechanistic origin than that for G10A and G11C. Since position 85 is downstream of the Alt P1/Alt 2 pairings, G85C cannot work by directly destabilizing Alt P1. Instead, G85C can potentially form a base-pair with G10 and strengthen the native P2 pairing in I_2 resulting in a native P1 and Alt 2 (Figure 1).

Since the G85C mutant appears to favor the I_2 intermediate with Alt 2, and the C14G and C15A mutants favor the I_1 intermediate with Alt P1, we

prepared double mutants to test whether G85C would lead C14G and C15A to favor I_2 . Indeed, the reactivities of the C14G:G85C and C15A:G85C double mutants were found to be stimulated by the lengthened AS oligomer (Table 2). These results support the model wherein G85C switches the I_1/I_2 equilibrium to favor I_2 . Apparently, formation of a native P1 (and faster folding) can be achieved either by weakening misfolds sequestering upstream pseudoknot-forming nucleotides (as in G10A and G11C), or by strengthening native interactions with downstream pseudoknot-forming nucleotides (as in G85C). Overall, these observations support the existence of Alt 2 in I_2 , and its being mutually exclusive with Alt P1.

The cleavage activities of the wild-type ribozyme in the presence of AS(-30/-7) and AS(-30/-3) were compared. The reaction kinetics were biphasic in the presence of both AS oligomers (Figure 2(a), Table 2 and data not shown). The burst amplitude was not affected by the length of the AS oligomer, suggesting the factors that determine population of I_1 and I_2 do not involve the -30 to -3 region. (Relative populations of I_1 and I_2 may involve interactions in P2; see Discussion.) However, the rates of the slow and burst phases were affected in opposite directions. The rate of the slow phase decreased by about twofold, while the rate of the burst phase increased by about twofold (Table 2). The increase in the rate of the burst phase, similar to G10A and G11C, supports the model wherein the burst phase of the wild-type ribozyme originates from I_2 and Alt 2 interferes

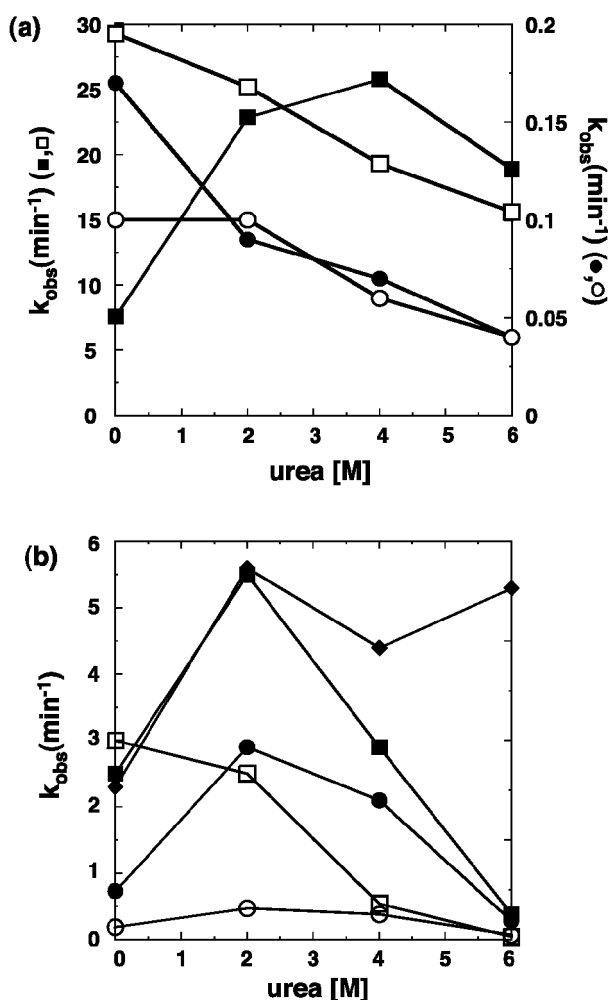


Figure 3. Dependence of the self-cleavage reaction on urea concentration. Observed rate constants are provided in Table 2. (a) Urea-dependence of wild-type and G11C ribozymes in the presence of different AS oligomers. Symbols are as follows: reactions in the presence of AS(-30/-7) for wild-type slow phase (●) and G11C (■), reactions in the presence of AS(-30/-3) for wild-type slow phase (○) and G11C (□). Data for the wild-type ribozyme refer to the right-hand y -axis, and data for G11C refer to the left-hand y -axis. (b) Urea-dependence of C14G (○), C15A (□), G85C (◆), C14G/G85C (●), and C15A/G85C (■) mutants, in the presence of AS(-30/-7).

with folding, while the decrease in rate for the slow phase suggests this phase of the wild-type ribozyme originates from a different intermediate and Alt 2 assists its folding.

Testing the Alt 3 helix with RNA mutations

The Alt 3 pairing is common to I_1 and I_2 , and involves ribozyme sequence only. Five individual positions in, or adjacent to, Alt 3 were mutated to test this pairing (Figure 1). Positions 26 and 27 are

unique, in that these do not appear to make important contributions to the native fold of the genomic ribozyme, and the antigenomic ribozyme does not have a U27 counterpart.²⁵ In the crystal structure of the self-cleaved genomic ribozyme, C26 and U27 are extruded and not well-ordered.²⁶ In addition, chemical modification experiments on the self-cleaved genomic ribozyme revealed modification of C26 and U27 on their Watson-Crick base-pairing faces.³⁴ Thus, deletion or modification of C26 and U27 was not expected to affect the native fold adversely; however, these changes were expected to destabilize Alt 3. Three mutants were made in Alt 3₅: C26 Δ , U27 Δ and U27A. When the predicted folds of residues 14-30 for this set of mutants were examined by free energy minimization using *mfold* 3.1, the lowest free energy structures revealed a native P3 pairing in place of Alt 3. (The predicted fold for U27A showed a base-pair formed between U20 and A27; however, this UA pair may not compete significantly with the native state, since U20 forms an extensive stacking network with G25 and G28 in the crystal structure.²⁶) Results from self-cleavage experiments on these three mutants were consistent with these expectations, as extensive cleavage of the ribozyme occurred during transcription (Table 1). These results support the existence of the Alt 3 pairing (Figure 1), and suggest that destabilization of Alt 3 favors the native ribozyme fold. This may be because P2₅ is now accessible for pairing, allowing P2 to form readily. Also, these results support the unimportance of residues C26 and U27 in the native fold, as expected.^{26,34}

To test Alt 3 further, a series of changes were made in Alt 3₅. These changes included C14G and C15A, which affect the stability of both Alt 3 and P2, and were thus expected to have more complex effects. Two other mutants were prepared to test effects on P2 and Alt 3 stability, C13A and C13G. C13G was predicted to result in a more stable Alt 3 pairing by forming an additional GC pair, whereas C13A was predicted to not affect Alt 3 (Table 1).

Mutations in Alt 3₅ had several effects on the self-cleavage reaction. Both C13A and C13G were slow-reacting; however, the rate of C13A was down only tenfold, while that of C13G was down 2800-fold (Table 1). The very slow rate of C13G is consistent with strengthening of Alt 3 and connecting of Alt 3 and Alt P1 into one large alternative pairing (see I_1 in Figure 1). In addition, C13G was predicted to have a destabilized P2 pairing, although a GG mismatch is only slightly destabilizing.³⁵ The tenfold slower rate of C13A is consistent with a weakening of P2 by replacement of a central CG base-pair with an AG mismatch. Also, since the rate decrease for C13A is much less than that for C13G, this supports position 13 being opposite C30 in I_1 (Figure 1). To test P2 disruption by C13A, the C13A:G82U double mutant was prepared to restore base-pairing in P2. Indeed, C13A:G82U reacted fourfold faster than C13A alone (Table 1), consistent with restoration of P2.

The C13A:G82U double mutant still reacted 2.5-fold slower than the wild-type ribozyme, which could be due to substitution of a CG base-pair with a weaker AU pair and lack of disruption of any alternative pairings. The ribozyme with the G82U change alone, which replaced a central CG base-pair in P2 with a CU mismatch, reacted four-fold slower than the wild-type and twofold slower than C13A:G82U (Table 1), consistent with the importance of having a stable P2 in the native fold. Overall, these mutants suggest that strengthening Alt 3 and weakening P2 both affect folding adversely.

The C14G ribozyme exhibited near-wild-type activity with an identical biphasic kinetic pattern (Table 1). This might result from compensatory effects of a favorable destabilization of Alt 3 and a modest destabilization of P2. To test this idea, a compensatory G to C change was made at position 81, which is the base-pairing partner of position 14. The G81C change alone decreased cleavage by threefold, similar to the G82U change and as expected for destabilization of P2. The C14G:G81C double mutant, however, was very reactive and cleaved during transcription. Thus, it appears that Alt 3 can be weakened by changes in either its downstream or upstream strands, as long as the stability of the native fold either is unchanged or is restored by a compensatory change.

The C15A ribozyme was unusual among the mutants in Alt 3₅, in that this single mutant had a significantly favorable effect on the rate. For example, the C15A ribozyme reacted 15-fold faster than C14G (Table 1). C15 participates in the penultimate base-pair of Alt 3, while C14 participates in the last base-pair of Alt 3 (Figure 1). Thus, breaking the internal C15/G28 base-pair may also destabilize the C14/G29 pair, in effect destabilizing two CG base-pairs with one change. The stability of P2 in the C15A ribozyme may still be somewhat compromised by the resulting AG mismatch. To test this idea, G80U single and C15A:G80U double mutants were prepared. The G80U change alone decreased cleavage by 1.7-fold, as expected for destabilization of P2. However, the C15A:G80U double mutant was very reactive and cleaved during transcription, similar to C14G:G81C.

To confirm that the Alt 3 ribozyme mutants were in fact reacting rapidly, a representative Alt 3-disrupting mutant, U27 Δ , was isolated as the precursor in sufficient quantities for rapid-mixing experiments. Preparation of uncleaved U27 Δ was accomplished by transcription at a lower temperature (30 °C for four hours). Rapid-mixing self-cleavage assays of U27 Δ with AS(-30/-7) revealed a burst-phase of 40% with a rapid rate of 39.0 min⁻¹ (Table 1). This result provides quantitative support for the ability of Alt 3 to inhibit the overall rate of ribozyme folding.

In summary, mutations support the existence of Alt 3 as a pairing that decreases the rate of folding. Mutations in either strand of Alt 3 that decrease its thermodynamic stability led to increased rates of

cleavage as long as native pairings were either unaffected or restored by compensatory changes. Conversely, mutations that strengthened Alt 3 alone led to slower rates of cleavage. Similarly, mutations that weakened P2 alone led to slower cleavage, while mutations that strengthened P2 led to faster cleavage. These results suggest that formation of the P2 pseudoknot can lead to rapid overall folding.

The effect of urea on the rate of cleavage

The effects of urea on RNA folding have been studied in various nucleic acid systems, including the RNase P ribozyme and model duplexes, and urea has been shown to facilitate the overall rate of RNA folding when disruption of alternative or premature native RNA interactions is at least partially rate-limiting.^{13,15,16,36,37} The effects of urea on the cleavage kinetics of several HDV ribozyme mutants were examined using AS(-30/-7)- and AS(-30/-3)-stimulated reactions (Table 2).

Self-cleavage of G11C was stimulated threefold by 2 M urea for the reactions carried out in the presence of AS(-30/-7) (Table 2, Figure 3(a)). However, 2-6 M urea provided no rate stimulation for the reaction of G11C in AS(-30/-3), and the urea-dependence was independent of AS oligomer length in this range. Based on our model, there are two alternative pairings, Alt 2 and Alt 3, present for both G10A and G11C in I₂ (Figure 1). Urea may serve to accelerate overall folding by increasing the unfolding rate of the Alt 2 pairing; if so, this might explain the lack of urea stimulation in the presence of AS(-30/-3), which also acts to break the Alt 2 pairing. This result suggests that urea could favor Alt 2 unfolding without compromising the stability of the native ribozyme interactions. Increased rate of Alt 2 unfolding may allow for capture of P1.1₃ by P1.1₅, which is accessible in the loop of Alt 3 (see Discussion).

Since Alt 3 is predicted in I₂, lack of urea-stimulation for G11C plus AS(-30/-3) implies that urea does not favor the rearrangement of Alt 3 to P3 and P2. According to the secondary structure models in Figure 1 in which P2 folding is initiated in I₂, the Alt 3 rearrangement essentially involves a trading of base-pairs. If this process is in rapid equilibrium or Alt 3 in I₂ is less extensive than shown, further increase in the kinetics of the rearrangement by urea should not affect the overall rate of folding and cleavage. As observed for larger ribozymes,¹⁶ the absence of urea stimulation for G11C with AS(-30/-3) is suggestive of kinetic trap-free folding, although the folding pathway appears to still have equilibrium intermediates that decrease the fraction of the ribozyme in the native fold.

The dependence of the burst phase of the wild-type ribozyme on urea and AS oligomer length showed striking similarity to G11C. In the presence of AS(-30/-7), the rate of the burst phase was stimulated twofold by 2 M urea to 24 min⁻¹, simi-

lar to the value of 23 min^{-1} measured for G11C under these conditions (Table 2). Moreover, the rate of the burst phase was not stimulated by 2–6 M urea in the presence of AS(–30/–3), and the urea-dependence was independent of AS oligomer length in this range, as observed for G11C. The cleavage rates for the wild-type burst phase and G11C ribozymes were nearly identical for AS(–30/–3) conditions. These results support the model wherein the burst phase of the wild-type originates from the I_2 intermediate.

Unlike G11C, wild-type slow phase and C15A ribozymes were not stimulated by urea for reactions with AS(–30/–7) or AS(–30/–3) (Table 2, Figure 3). The slow phase of the wild-type ribozyme contains Alt P1 and Alt 3. As discussed above, urea does not appear to favor exchange of Alt 3 for native pairings, while Alt 2 may assist folding of the wild type slow phase based on 2 M urea inhibiting folding in AS(–30/–7) but not AS(–30/–3) (see Discussion). C15A might be expected to be stimulated by urea, as Alt 3 has been disfavored and Alt P1 is present. However, C15A has a P2 pairing with compromised stability that might be especially sensitive to destabilization by urea. Supporting this idea, the rate of cleavage of C14G was stimulated about threefold by urea. C14G leads to a G-G mismatch in P2, which has been shown to have a ΔG_{37}° of -2.6 kcal/mol in a similar context.³⁵ Thus, the G-G mismatch-containing P2 in C14G appears to provide sufficient stability to allow urea to stimulate the reaction without compromising the stability of the native fold. Since the reactivity of C14G is not stimulated by the lengthened AS oligomer, this mutant likely originates from an I_1 intermediate lacking Alt 3. This model would suggest that urea stimulates rearrangement of Alt P1 to the native fold. As with Alt 2, Alt P1 sequesters the downstream strand of P1.1, as well as a portion of the upstream strand of P2. The stimulatory effect of urea on the C14G mutant may reflect faster unfolding of Alt P1, which allows for capture of the pseudoknot strand P1.1_{3'} or P2_{5'} or both.

The G85C ribozyme is predicted to have a stable P2. Indeed, urea led to an approximately twofold stimulation of the cleavage rate by G85C with both AS(–30/–7) and AS(–30/–3) that may be due to breaking of Alt 2 or Alt P1 or both if a mixture of I_1 and I_2 are occupied for G85C (Table 2, Figure 3(b)). Lack of rate stimulation by urea for C15A was attributed to compromised stability of the resulting P2 pairing (see above). To test this idea, the urea-dependence of the C15A:G85C double mutant was examined (Table 2, Figure 3(b)). As predicted, urea now stimulated the reaction, with a approximately twofold increase in rate from 0 to 2 M urea with both AS(–30/–7) and AS(–30/–3). The urea effects on the C15A and C15A:G85C mutants indicate that urea can fail to stimulate folding in cases where the native structure is not sufficiently stable to withstand the urea treatment. This provides a case for which absence of urea

stimulation does not reflect trap-free folding. Rate stimulation by urea for G85C-containing ribozymes in the presence of AS(–30/–3) may reflect partial occupancy of I_1 by the ribozymes, also the rate never equals that of G11C or the wild-type burst phase.

In summary, urea stimulated the rate of ribozyme cleavage when either Alt 2 or Alt P1 was present. Common to Alt 2 and Alt P1 is sequestration of a strand of one or both pseudoknots, and the rate of melting of these pre-formed structure may limit overall folding. In addition, urea stimulation required that the pairings in the native fold have sufficient stability to maintain efficient folding in the presence of the denaturant.

Discussion

The genomic HDV ribozyme is a small catalytic RNA of approximately 85 nucleotides that contains complex secondary and tertiary structures. There are five native pairings in the ribozyme, and two of these form pseudoknots, P2 and P1.1. Pseudoknots involve base-pairing between nucleotides embedded in a stem-loop, such as a hairpin loop, a bulge, or an internal loop, and nucleotides outside the stem-loop. Since RNA will typically form local interactions before long-range interactions, folding of pseudoknots can be slow if one of the strands is prone to sequestration in an alternative local fold. In this study, we demonstrated that the genomic HDV ribozyme initially folds into one of two incorrect secondary structures containing multiple alternative pairings, and missing both pseudoknots. We tested these pairings by examining the reactivity of ribozyme mutants that modulate the stability of the alternative pairings while maintaining the native structure of the ribozyme. Correct folding of the ribozyme is attenuated by each of three alternative pairings, and all of these alternative pairings limit the rate at which the native pseudoknot pairings form. Here, we present several models that explain the equilibrium and kinetic effects observed.

Presence of alternative pairings and modeling their effects on native folding

Free energy minimization of the secondary structure of the ribozyme suggested that three major alternative pairings could form in the presence of AS oligomers. Two of these, Alt 2 and Alt 3, were previously identified by structure mapping experiments of a precursor form of the ribozyme.³² An Alt 3 pairing was identified by structure mapping experiments on 3'-truncated versions of the self-cleaved genomic ribozyme.³⁸ The third of these alternative pairings, Alt P1, was not identified by structure mapping experiments. However, the 60% of the wild-type ribozyme that partitions to the Alt P1-containing intermediate, I_1 , does not contain significantly more single-stranded nucleotides than I_2 , making its identification by single-stranded

ribonucleases problematic (Figure 1). In addition, the 30% of the ribozyme that partitions to I_2 is cleavable in part of the region comprising Alt P1, contributing a positive signal to structure mapping and compounding the problem of distinguishing Alt P1 by structure mapping. The double-stranded RNA-specific nuclease V1 did cleave most of the nucleotides in Alt P1 at least lightly, supporting formation of the Alt P1 pairing in a subpopulation of the ribozyme.³² Each of the three proposed alternative pairings was tested by site-directed mutagenesis and kinetic characterization.

The relationship between the rate of self-cleavage and RNA folding requires consideration. RNA folding pathways typically require a series of intermediates, and branched pathways that are non-productive can be populated. We predicted a number of alternative pairings and tested them functionally in this study by determining the activity of single and double mutant ribozymes. Nucleotides essential to tertiary structure formation, based on the crystal structure, were not modified and the native secondary structure was either unchanged or restored; as such, observed cleavage rates are interpreted in terms of the fraction of the ribozyme correctly folded.

We assume the following simple model, in which $k_{\text{obs}} = f_{\text{native}} \times k_{\text{int}}$, where k_{obs} is the observed rate constant for cleavage, k_{int} is the intrinsic rate constant for cleavage, which is rapid ($>39 \text{ min}^{-1}$, see below), and f_{native} is the fraction of the ribozyme that is folded in the native conformation. The fraction of the ribozyme in the native fold is limited by the internal equilibrium constants for Alt P1, Alt 2, and Alt 3. Since Alt 3 is common to I_1 and I_2 , and Alt P1 and Alt 2 are mutually exclusive, the following expression can be written for the fraction of the total ribozyme folded correctly:

$$f_{\text{native}} = [1 - (f_{\text{Alt P1}} + f_{\text{Alt 2}})](1 - f_{\text{Alt 3}})$$

where f_{native} accounts for secondary structure formation; tertiary structure formation equilibria could add more terms that would reduce the value of f_{native} further, although the present experiments do not address this possibility. This expression assumes that folding of Alt 3 is independent of Alt 2 and Alt P1. According to the model in Figure 1, for all constructs:

$$f_{\text{Alt 3}} = [\text{Alt 3}]/([\text{Alt 3}] + [\text{N}_{\text{Alt 3}}])$$

where $\text{N}_{\text{Alt 3}}$ represents the native interactions of all Alt 3-forming nucleotides. For constructs in which I_1 is the dominant intermediate:

$$f_{\text{Alt P1}} = [\text{Alt P1}]/([\text{Alt P1}] + [\text{N}_{\text{Alt P1}}])$$

where $\text{N}_{\text{Alt P1}}$ represents the native interactions of all Alt P1-forming nucleotides, and k_{obs} reduces to:

$$k_{\text{obs}} = k_{\text{int}}/[(1 + K_{\text{Alt P1}})(1 + K_{\text{Alt 3}})]$$

The internal equilibrium constants (K) are for mis-

folding, and

$$K_{\text{Alt P1}} = [\text{Alt P1}]/[\text{N}_{\text{Alt P1}}]$$

and

$$K_{\text{Alt 3}} = [\text{Alt 3}]/[\text{N}_{\text{Alt 3}}].$$

Likewise, for constructs in which I_2 is the dominant intermediate:

$$f_{\text{Alt 2}} = [\text{Alt 2}]/([\text{Alt 2}] + [\text{N}_{\text{Alt 2}}])$$

where $\text{N}_{\text{Alt 2}}$ represents the native interactions of all Alt 2-forming nucleotides. k_{obs} reduces to:

$$k_{\text{obs}} = k_{\text{int}}/[(1 + K_{\text{Alt 2}})(1 + K_{\text{Alt 3}})]$$

where,

$$K_{\text{Alt 2}} = [\text{Alt 2}]/[\text{N}_{\text{Alt 2}}]$$

These expressions for k_{obs} involve binding polynomials; therefore, fold-reduction in observed rate constant for mutant ribozyme self-cleavage could be interpreted in terms of internal equilibrium constants. For example, if a tenfold rescue in cleavage rate is found for an Alt 3-breaking mutation, then:

$$10/1 = (1 + K_{\text{Alt 3,slow}})/(1 + K_{\text{Alt 3,fast}})$$

If $K_{\text{Alt 3,fast}} \ll 1$, then $K_{\text{Alt 3,slow}}$ is approximately 9 for the slow-folding construct. In practice, the observed rate constant can be decreased if kinetic traps are present. For example, the equilibrium constant for formation of an alternative pairing might be only three; however, if unfolding of the pairing is slow, then the fold-decrease in k_{obs} may be substantially more than four. In either case, fold-reductions in k_{obs} can be attributed to population of non-reactive folds, since the native fold of the ribozyme is known and was either unchanged or restored.

Testing of predicted alternative pairings was greatly aided by knowledge of the native fold of the ribozyme. The secondary structure of the ribozyme in solution was worked out in a number of studies, largely from the Been laboratory,³⁹⁻⁴¹ and then confirmed and extended by solving of the crystal structure of the self-cleaved form of the ribozyme.²⁶ Revealed in the crystal structure was the two base-pair pairing, P1.1, which is part of a pseudoknot. Formation of P1.1 in the reactive form of the ribozyme in solution was subsequently confirmed by self-cleavage studies with a series of mutants.⁴¹

Formation of Alt P1 in I_1 was tested with the ribozyme mutants, G10A and G11C. Both mutants were predicted to destabilize Alt P1 in I_1 (Figure 1), and their 34 to 42-fold faster rates (Table 1) were consistent with this model. The $\Delta\Delta G_{37}^\circ$ calculated by *mfold* for the I_1 to I_2 equilibrium for the wild-type ribozyme favored I_1 by 4.1 kcal/mol.^{20,33} This calculated ΔG_{37}° predicts that G10A and G11C should be ≈ 775 -fold faster than wild-type. The

actual increase in rate, although substantial, is ≈ 20 -fold less than predicted. This discrepancy could be due to formation of ≈ 3 bp in the active-site-distal portion of P2 in I_2 (Figure 1) that was not accounted for in the prediction, or to uncertainty in the predicted $\Delta\Delta G_{37}^\circ$, since thermodynamic rules for complex internal loops are only partly worked out.²⁰

The G11C mutant was predicted to favor Alt 2 in place of Alt P1. Presence of the Alt 2 pairing was confirmed by fourfold faster reactivity of G11C in the presence of the longer AS oligomer, AS (-30/-3) (Table 2). Similar three- to fourfold rate increases with AS(-30/-3) were found with G85C and C14G:G85C. These observations suggest that the internal equilibrium constant favoring Alt 2 over $N_{\text{Alt } 2}$ is ≈ 2 to 3. This modest value is consistent with Alt 2 having only three base-pairs, which are traded for two of the same type of base-pairs.

Formation of the third alternative pairing, Alt 3, was tested by a set of mutants that weakened the pairing, involving changes in both the 5' and 3'-strands of Alt 3 (Table 1). Fast-folding mutants that destabilized Alt 3 without affecting the native fold led to faster cleavage, which was typically realized in co-transcriptional cleavage (see C26 Δ , U27A, U27 Δ , C14G:G81C and C15A:G80U). A lower limit to the fold-increase was estimated from consideration of C15A, which destabilized Alt 3 with a sub-optimal P2. The C15A mutant ribozyme reacted 13-fold faster than the wild-type slow phase, suggesting that the co-transcriptional reacting mutants react more than 13-fold faster. Moreover, the precursor form of U27 Δ was prepared under special transcription conditions and found to fold fast with a burst phase of 39.0 min^{-1} with AS(-30/-7), \approx threefold faster than the wild-type burst phase. This analysis suggests that the internal equilibrium constant for Alt 3 over $N_{\text{Alt } 3}$ is ≈ 2 to 3. The Alt 3 pairing has five base-pairs, with two GC pairs at either end, which may account, in part, for its stability.

Co-transcriptional cleavage of any -30/99 construct is somewhat surprising, based on the possibility of forming the inactivating Alt 1 pairing between the inhibitory stretch -24/-15 and P2_{3'}.³² One possible explanation is that P2_{3'} partitions between long-range pairings with the upstream inhibitory stretch and P2_{5'} nucleotides accessible in the Alt 3 mutants. If so, early formation of the P2 pseudoknot pairing can drive overall folding. For folding of the wild-type (-30/99) ribozyme during transcription, P2_{5'} may form the local Alt 3 or Alt P1 pairings much faster than P2, leaving P2_{3'} to form the long-range Alt 1 and preventing significant formation of the native fold in the absence of an AS oligomer. While formation of P2 appears to be fairly rapid at $>30 \text{ min}^{-1}$ (see below), simple close-range stem-loops such as Alt 3 and Alt P1 typically form with time constants of $< 10 \text{ }\mu\text{s}$.⁴²

Many of the inhibitory effects of alternative pairings can be explained by the simple equilibrium

model above. The key feature of this model is that the intrinsic rate of chemistry is masked by a shift in the equilibrium population of ribozyme toward misfolds. (The position of the rate-limiting step is discussed in the next section.) It is unclear whether any of the mutants studied here, even the fastest-folding ones, have a significant fraction of the uncleaved ribozyme molecules in the native fold. This problem arises because of the large number of alternative pairings possible, and that even when native secondary structure forms, tertiary structure unfolding may be rapid relative to chemistry (see next section), causing the tertiary fold to be poorly populated. Lack of significant amounts of native fold in the uncleaved population indicates that caution should be exercised in interpreting structural or dynamic studies designed to directly assay the uncleaved native state. Exceptions to this may be if the data is obtained through measurements of the rate of self-cleavage, which can, depending on conditions, assay the rare native state. This may explain why a pK_A near neutrality was not found by direct measurements on the uncleaved genomic HDV ribozyme by Doudna and co-workers, and those authors also suggested related scenarios.⁴³

The fastest cleavage rate of 39 min^{-1} observed here is similar to the rate of 23 min^{-1} , observed for an HDV antigenomic ribozyme with a shortened P4 under similar reaction conditions without denaturant.⁴⁴ These values are lower limits for the intrinsic rate of chemistry. Similar values for the genomic and antigenomic ribozymes are consistent with similar secondary structures, and the likelihood of similar mechanisms for tertiary folding and cleavage, as proposed based on kinetic studies.^{45,46}

Different fast-folding mutants have different mechanistic origins

In previous reports, several large RNAs have been prepared that fold rapidly and avoid some or all kinetic traps.^{6,9,10,13-17} Success in preparing fast folders in large RNAs suggested that it may also be possible to do so with the smaller HDV ribozyme. Indeed, several different fast-folding ribozymes were prepared in this study, including mutants that weakened Alt P1, weakened Alt 3, and broke Alt 2 (Tables 1 & 2). In addition, G85C mutants led to faster folding, but appeared to do so by strengthening native interactions in P2. Results from the crystal structure implicated base-pairing of G10 with a cytosine base at position 85, although the G10 interactions were with a cytosine from a neighboring molecule in the crystal.⁴⁷ This base-pairing arrangement would lead to a 7 bp P2 helix. Improved reactivity with increased P2 length has been suggested in other contexts,^{48,49} although we are unaware of demonstration of the importance of lengthening P2 from 6 to 7 bp. The enhanced cleavage rate of G85C suggests that a J1/2 of only 2 nt is sufficient for reactivity.

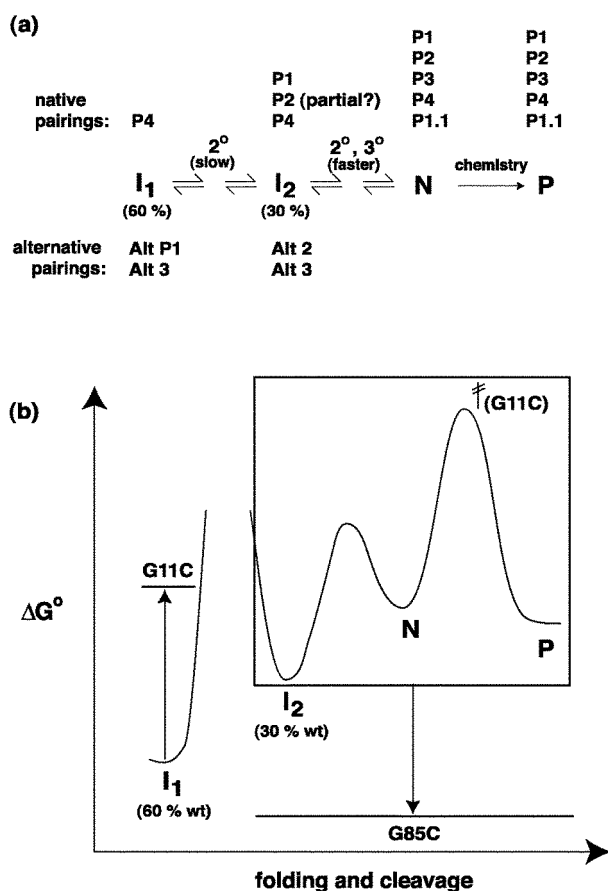


Figure 4. (a) Kinetic model for folding of the genomic HDV ribozyme from intermediates I_1 and I_2 . The alternative and native pairings present in each fold based on experimental data are given. Early in the reaction, 60% of the wild-type RNA exists in the I_1 conformation, and 30% in I_2 . Both intermediates contain non-native secondary structures; however, I_1 is slower-reacting than I_2 , presumably because Alt P1 is especially stable and I_1 has fewer native pairings. The I_1 to I_2 conversion was found to be slow and to be limited by rearrangement of Alt P1 to P1. Folding from I_2 to N involves secondary and tertiary folding events, and their order of occurrence is not clear. Only the native state, N, can lead to cleavage and product, P. (b) Free energy profile for the folding and cleavage reaction of the wild-type HDV ribozyme and the mutants G11C and G85C. The mutants accelerate the folding reaction by distinct mechanistic strategies. G11C destabilizes Alt P1, which disfavors the I_1 conformation, but maintains a stable P2 in all other conformations. This effect is depicted in the profile by a raising of the free energy of the I_1 state. G85C stabilizes P2, which should favor I_2 , N and P, as well as the transition states between these species, since P2 is expected to be present in all of these states. This effect is depicted in the profile by a lowering of the free energy of a box containing all these states. I_2 may partition to N over returning to I_1 based on the wild-type ribozyme displaying biphasic kinetics despite I_1 being significantly more stable than I_2 . The rate-limiting step within the box for G11C is shown as chemistry (double-dagger G11C) based on solvent isotope and pH studies in the G11C + AS(-30/-7) background.^{45,53,54} We have not tested if chemistry is the rate-limiting step for other RNAs, so the height of the barrier(s) between I_1 and I_2 is not drawn. The uncleaved N state is shown slightly

A kinetic model for folding of the G11C, G85C, and wild-type ribozymes is presented in Figure 4. The sets of native and alternative pairings present in I_1 , I_2 , N, and P are shown in Figure 4(a). The G11C change destabilizes Alt P1 in I_1 , but is not expected to destabilize I_2 , N, or P significantly, since a stable P2 is predicted (see above)(Figure 4(a)). On the basis of this model, G11C is depicted as higher in free energy than wild-type for I_1 , but I_2 , N, P, and their transition states are expected to be essentially unchanged in free energy (Figure 4(b)). In contrast, the G85C change stabilizes P2 present in I_2 , N, and P, but not in I_1 , since its base-pairing partner, G10, is sequestered in Alt P1. Enhanced stability of the native state for G85C is evinced by the stability of G85C in 6 M urea, whereas other mutants and the wild-type are inhibited by 6 M urea (Table 2). On the basis of this model, G85C is depicted as lower in free energy than the wild-type for I_2 , N, P, and their transition states, but not for I_1 (Figure 4(b)). The outcome of these two different effects is similar in that folding for G11C and G85C is predicted to occur within the I_2 , N, and P states, boxed in Figure 4(b). This is consistent with enhanced rates of cleavage for the G11C and G85C mutants, although G11C is somewhat faster than G85C with both AS oligomers, suggesting that weakening Alt P1 by the G11C change may be more effective at favoring I_2 over I_1 than strengthening P2 with the G85C change. Folding of I_2 to the native state involves large-scale conformational changes at both the secondary and tertiary structural levels. The order and number of distinct secondary and tertiary structure formation steps is uncertain (Figures 1 and 4), and it remains possible that formation of some tertiary structure precedes, and possibly assists, complete formation of secondary structure, as observed in other systems.⁵⁰⁻⁵²

We previously characterized the effects of pH, Mg^{2+} , and 2H_2O on the reactivity of the G11C mutant.^{45,53,54} These studies were consistent with the notion that the rate-limiting step for G11C cleavage is the chemical step (based on pH and 2H_2O effects) and supported a model involving two proton transfers in the rate-limiting step, C75 as the general acid for phosphodiester bond cleavage with a pK_A near neutrality, and hydrated magnesium hydroxide as the general base under physiological Mg^{2+} concentrations. The kinetic model in Figure 4 shows folding of I_2 to N involving rearrangements of secondary and tertiary structure, followed by N cleaving to form P in the rate-limiting chemistry step. Chemistry can be the rate-limiting step for cleavage, even in the presence of

higher in free energy than the cleaved P state, based on ground state destabilization between protonated C75 and a catalytic Mg^{2+} .^{45,53}

folding steps that are slower than chemistry, if I_2 and N are in rapid equilibrium (i.e. N unfolds faster than it cleaves). This would be the case if the native state is inherently unstable. Prior studies revealed anticooperative interaction between protonated C75 and metal ion,⁴⁵ which may destabilize the native fold of the precursor.

It is possible that the identity of the rate-limiting step changes with pH. For example, since the rate of G11C cleavage increases log-linearly with pH,⁴⁵ it is possible that at high pH values the height of the N to P barrier falls below that of the I_2 to N barrier, which would lead to a kinetic pK_A (i.e. a pK_A that is not due to binding of a proton to C75). If this were indeed the case, then the true pK_A of C75 would be greater than neutrality, and shifted even further from its unperturbed value of 4.2. Nevertheless, we disfavor a model in which the pK_A is kinetic in origin, on the basis of experiments suggesting that chemistry is rate-limiting in the plateau region of the pH-profile. (There is a substantial (about fourfold) kinetic solvent isotope effect in the plateau region of the pH-profile, and proton inventory experiments in the plateau region support two proton transfers as rate limiting.^{45,54}) It is presently unclear whether the rate-limiting step is chemistry for the mutants that fold from I_1 ; therefore, the height of the I_1 to I_2 barrier is not shown explicitly in Figure 4(b).

In a survey of 21 genomic HDV isolates,^{25,32} position 85 was occupied overwhelmingly by C (19 out of 21 isolates), although it was G in the wild-type sequence chosen here from a human with acute δ -hepatitis.⁵⁵ In addition, only three of the 21 isolates had mutations in Alt 3-forming nucleotides, and these occurred at positions 26 and 27. The low frequency of Alt 3-breaking mutations is somewhat surprising, given that nucleotides 26 and 27 are not important to cleavage (Table 1), or to the native structure of the ribozyme.^{26,34} Also, positions 10 and 11 were found to be G in all 21 isolates. It appears that HDV achieves faster folding *in vivo* by strengthening native interactions rather than weakening non-native ones. It is not clear why non-native interactions are not weakened *in vivo* to achieve faster folding. One possibility is that folding is fast enough to allow cleavage *in vivo*, or that folding is assisted by chaperones. Another possibility is that sequences involved in alternative pairings in the ribozyme are under selective pressure to form other non-ribozyme RNA structures, such as the rod form of the ribozyme, which carry out critical biological functions for the virus such as replication and packaging. Also, strengthened native structure may slow invasion by the attenuator sequence and allow time for extensive ribozyme cleavage during transcription (A. D. Parente & P.C.B., unpublished results).

The wild-type ribozyme displayed biphasic kinetics with $\approx 60\%$ reacting in a slow phase and $\approx 30\%$ reacting in a burst phase. The fast-reacting phase showed characteristics similar to the G11C

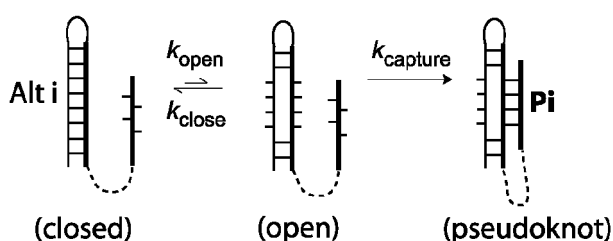
ribozyme, including rate of cleavage, urea-dependence, and AS oligomer length dependence. These observations suggest that the wild-type ribozyme partitions into I_1 and I_2 . I_1 was predicted to be 4.1 kcal/mol more stable than I_2 (see above), and the slow phase of the wild-type reaction was found to be 70 times slower than the burst phase, consistent with a stable I_1 intermediate. Based on the I_1 stability and the binding polynomial model developed in the preceding section, we expected that the amplitude on the burst phase of the wild-type ribozyme might be considerably smaller than 30%. One possible reason for the substantial burst phase is that I_2 is not in rapid equilibrium with I_1 . Perhaps folding of I_2 toward N is faster than rearrangement of pairings to go back to I_1 , allowing kinetic partitioning and the I_2 intermediate to be observed as a sizeable burst (Figure 4(b)). This situation may arise if, for example, rearrangement of P2 involving residues 82-84 (or 85) with 13-11 (or 10) is rapid and captures I_2 preventing its escape back to I_1 . The stimulatory effect of urea on certain mutants suggests that this might indeed occur (see the next section). Thus, preparation of the initial states may be critical to the outcome of the reaction.

A capture mechanism for pseudoknot formation

We examined the effect of the chemical denaturant urea on the rate of cleavage for several of the mutants. Rates were measured at 0, 2, 4, and 6 M urea, and increases and decreases in rate were observed. Urea was found to enhance cleavage of G11C and wild-type (burst phase) ribozymes, as well as G85C-containing mutants. For G11C and the wild-type burst phase this enhancement was lost in the presence of the Alt 2-breaking AS(-30/-3) oligomer. Thus, faster folding of these ribozymes may arise from an increased rate of unfolding of the Alt 2 pairing in the presence of urea which releases P1.1₃. The P1.1₅ strand is single-stranded in the loop of Alt 3 based upon structure mapping.³² Similar behavior may occur for the P2 pseudoknot based upon the urea enhancement of the C14G mutant, which appears to fold from the I_1 state containing Alt P1 and is not enhanced by AS(-30/-3).

The wild-type slow phase exhibited the opposite dependence on urea and AS oligomer length as the burst phase (Table 2). One explanation for this effect is that Alt 2 actually aids wild-type folding from I_1 to I_2 by providing stabilizing interactions for G38-40 outside of Alt P1 that slows its return to I_1 and allows time for P2 to form. Thus, it is possible that Alt 2 serves a productive role for folding of the slow phase wild-type ribozyme that is inhibitory in Alt P1-weakened mutants.

A rudimentary mechanism can be drawn that explains the effects of urea and AS oligomers on pseudoknot formation (Scheme 1). We model pseudoknot formation as unfolding or conformational



switching of an alternative pairing (Alt i) from a closed state to an open state, which can then be captured by the complementary strand of the pseudoknot to form pairing Pi. Capture is used, since the complementary pseudoknot strand can make the last step effectively irreversible if subsequent steps are fast (Figure 4(b)). For wild-type burst phase and G11C, urea and AS(-30/-3) can increase k_{open} for Alt 2 such that the overall folding rate of P1.1 increases. For wild-type slow phase, urea and AS(-30/-3) may increase k_{close} from an I₂-like state without any P2 formed, thus decreasing the population of the I₂-like state that can attempt P2 formation. This model is consistent with P2 forming before P1.1 for wild-type slow phase. This capture mechanism is similar to that proposed for other RNA folding events including ribonucleoprotein (RNP) assembly and folding of helix junctions.^{56,57}

A slow-folding pseudoknot has been observed in the Tetrahymena ribozyme, in which the P3 pseudoknot pairing is prone to alternative local folding in an Alt P3 pairing.¹³ In that case, slow-folding mutants were enhanced by urea, which may have acted to increase the rate of unfolding of one of the pseudoknot strands.¹³ Also, the *Escherichia coli* α mRNA pseudoknot has two conformers that interconvert with slow kinetics.⁵⁸ Studies on the folding of the P2 strand in the antigenomic ribozyme have been carried out by Been and co-workers, and an unusual role for a bulged adenosine base in the antigenomic P2/P2a pairing was proposed.⁵⁹ They observed that deletion of the adenosine base led to a steeper urea and temperature-dependence for self-cleavage, suggesting a model wherein the bulged A may serve to increase the rate of refolding from an inactive ribozyme structure. Thus, folding of pseudoknots may be difficult for large and small RNAs alike.

Reaction of G11C with AS(-30/-3) appears to be free of kinetic traps, thus providing lower limits for rates of tertiary structure formation and bond cleavage. (It is possible that urea concentrations between 0 and 2 M urea could lead to small rate accelerations; however, it is unlikely that such effects would be substantial in this small range of urea concentrations.) The rate of folding of the 255 nucleotide catalytic domain

from *Bacillus subtilis* P RNA, which appears to fold without kinetic traps, is 390 min^{-1} .¹⁶ The lower limit for the rate of tertiary structure folding measured here for the smaller HDV ribozyme is $\approx 39 \text{ min}^{-1}$ (Table 1). These two rates are within tenfold of each other, and may be even closer if tertiary folding of the fast-folding HDV ribozymes is faster than measured by cleavage, or is limited by non-native equilibrium intermediates yet to be identified. These comparisons indicate that small multiple pseudoknot-containing RNAs can fold rapidly. Fast-folding mutants should provide useful tools for probing the energy landscape for tertiary folding and bond cleavage by the HDV ribozyme.

Materials and Methods

Preparation of mutant RNA

The -30/99 wild-type RNA used in this study was transcribed from pT7 -30/99 using phage T7 polymerase, as described.³² This transcript contains 30 nucleotides upstream of the cleavage site and 15 nucleotides downstream of the 3' end of the ribozyme (Figure 1). Transcripts are *Bfa*I run-offs that contain ribozyme and viral-derived RNA sequence only. All mutant plasmids were generated from pT7 -30/99, using the Quik-Change kit (Stratagene). Sequences were confirmed by the dideoxy method after a miniprep purification (Qiagen). RNA was transcribed, purified and radiolabeled as described.³²

Ribozyme kinetics and data fitting

Hand-mixing kinetics

Reactions were performed in a fashion similar to those described.⁴⁵ A typical self-cleavage reaction contained $\approx 2 \text{ nM}$ 5'-end-labeled RNA, 25 mM Hepes (pH 8.0), 10 mM MgCl₂, and an antisense oligomer as appropriate. The RNA was renatured at 55°C for ten minutes in TE (10 mM Tris, 1 mM EDTA, pH 7.5), and placed at room temperature for ten minutes. Buffer was added followed by the addition of the appropriate AS oligomer (final concentration of 10 μM , which is saturating³²). The sequence of AS (-30/-7) is published,³² and the sequence of AS(-30/-3) is 5'-CAGGTAAGAAAGGATGGAACGCGGACCCACAC, which is complementary to RNA nucleotides -30 to -3. The mixture was incubated at 37°C for two minutes without MgCl₂, an aliquot was removed, and self-cleavage was initiated by the addition of MgCl₂ to 10 mM. The reaction was quenched by removing a 4 μl aliquot at a specific time, and adding 4 μl of a 95% (v/v) formamide loading buffer/20 mM EDTA quench. For all kinetic experiments, the quenched samples were fractionated on a denaturing 5% (w/v) polyacrylamide gel. The gels were dried and quantified by a Phosphorimager (Molecular Dynamics).

Urea-dependence of the wild-type and mutant RNA

The urea-dependence of self-cleavage was conducted by hand-mixing and rapid mixing as follows. The RNA was treated as described above, followed by the addition of Hepes (25 mM final, pH 8.0) and the appropriate AS

oligomer. Variable amounts of a 10 M urea stock solution were added to the reaction. The mixture was incubated at 37°C for two minutes without MgCl₂, an aliquot was withdrawn, and self-cleavage was initiated by the addition of a stock MgCl₂ solution to 10 mM.

Rapid-quench kinetics

Rapid-mixing experiments were performed on an RQF-3 chemical quench-flow apparatus (KinTek, State College, PA). The RNA was renatured in TE at 55°C and mixed with buffer and the appropriate AS oligomer, all to give 2× concentrations. An aliquot was withdrawn to serve as the time zero reading. The reaction was initiated by rapid mixing with a 2× solution of MgCl₂. Final conditions for the self-cleavage reaction were 25 mM Hepes (pH 8.0), 10 μM AS oligomer, and 10 mM MgCl₂ at 37°C. Urea-dependence measurements were done by including 1× urea in each of the syringes. The reaction was quenched by rapid mixing with 0.5 M EDTA to a final concentration of 0.3 M, and placed on solid CO₂. Aliquots were fractionated on a denaturing 5% polyacrylamide gel.

Data fitting

Plots of fraction product *versus* time were fit to the single-exponential equation:

$$f_c = A + B \exp(-k_{\text{obs}}t) \quad (1)$$

where f_c is the fraction of precursor ribozyme cleaved, k_{obs} is the observed first-order rate constant for ribozyme cleavage for the non-burst phase, t is time, A is the fraction of the ribozyme cleaved at completion, and $A + B$ is the burst fraction (present under some of the reaction conditions). The first time-point was taken at 15 seconds for hand-mixing and 0.1 second for rapid-mixing experiments. Kinetic parameters were obtained using non-linear, least-squares fitting by Kaleidagraph (Synergy Software).

Computer prediction of secondary structure

The secondary structure of the ribozyme plus flanking sequence was predicted by free energy minimization using the *mfold* 3.1 program of Zuker with the Turner rules^{20,33} (see <http://bioinfo.math.rpi.edu/~mfold/rna/form1.cgi>). The window size was set to 1 and percentage suboptimal to 20%. These settings allowed us to visualize secondary structures that the program otherwise considers too closely related to show.

Acknowledgments

We thank the members of the Cameron laboratory for use of their chemical quench-flow instrument, and Shuichi Nakano and members of the Bevilacqua laboratory for helpful comments. This work was supported by NIH grant GM58709, a fellowship from the Alfred P. Sloan Foundation and a Camille Dreyfus Teacher-Scholar Award.

References

- Doherty, E. A. & Doudna, J. A. (2001). Ribozyme structures and mechanisms. *Annu. Rev. Biophys. Biomol. Struct.* **30**, 457-475.
- Rupert, P. B. & Ferre-D'Amare, A. R. (2001). Crystal structure of a hairpin ribozyme-inhibitor complex with implications for catalysis. *Nature*, **410**, 780-786.
- Ban, N., Nissen, P., Hansen, J., Moore, P. B. & Steitz, T. A. (2000). The complete atomic structure of the large ribosomal subunit at 2.4 Å resolution. *Science*, **289**, 905-920.
- Yusupov, M. M., Yusupova, G. Z., Baucom, A., Lieberman, K., Earnest, T. N., Cate, J. H. & Noller, H. F. (2001). Crystal structure of the ribosome at 5.5 Å resolution. *Science*, **292**, 883-896.
- Cole, P. E. & Crothers, D. M. (1972). Conformational changes of transfer ribonucleic acid. Relaxation kinetics of the early melting transition of methionine transfer ribonucleic acid (*Escherichia coli*). *Biochemistry*, **11**, 4368-4374.
- Treiber, D. K., Rook, M. S., Zarrinkar, P. P. & Williamson, J. R. (1998). Kinetic intermediates trapped by native interactions in RNA folding. *Science*, **279**, 1943-1946.
- Sclavi, B., Sullivan, M., Chance, M. R., Brenowitz, M. & Woodson, S. A. (1998). RNA folding at millisecond intervals by synchrotron hydroxyl radical footprinting. *Science*, **279**, 1940-1943.
- Russell, R. & Herschlag, D. (2001). Probing the folding landscape of the Tetrahymena ribozyme: commitment to form the native conformation is late in the folding pathway. *J. Mol. Biol.* **308**, 839-851.
- Pan, T., Fang, X. & Sosnick, T. (1999). Pathway modulation, circular permutation and rapid RNA folding under kinetic control. *J. Mol. Biol.* **286**, 721-731.
- Buchmueller, K. L., Webb, A. E., Richardson, D. A. & Weeks, K. M. (2000). A collapsed non-native RNA folding state. *Nature Struct. Biol.* **7**, 362-366.
- Agalarov, S. C., Sridhar Prasad, G., Funke, P. M., Stout, C. D. & Williamson, J. R. (2000). Structure of the S15,S6,S18-rRNA complex: assembly of the 30 S ribosome central domain. *Science*, **288**, 107-113.
- Treiber, D. K. & Williamson, J. R. (1999). Exposing the kinetic traps in RNA folding. *Curr. Opin. Struct. Biol.* **9**, 339-345.
- Pan, J. & Woodson, S. A. (1998). Folding intermediates of a self-splicing RNA: mispairing of the catalytic core. *J. Mol. Biol.* **280**, 597-609.
- Pan, J., Deras, M. L. & Woodson, S. A. (2000). Fast folding of a ribozyme by stabilizing core interactions: evidence for multiple folding pathways in RNA. *J. Mol. Biol.* **296**, 133-144.
- Rook, M. S., Treiber, D. K. & Williamson, J. R. (1998). Fast folding mutants of the Tetrahymena group I ribozyme reveal a rugged folding energy landscape. *J. Mol. Biol.* **281**, 609-620.
- Fang, X., Pan, T. & Sosnick, T. R. (1999). Mg²⁺-dependent folding of a large ribozyme without kinetic traps. *Nature Struct. Biol.* **6**, 1091-1095.
- Webb, A. E. & Weeks, K. M. (2001). A collapsed state functions to self-chaperone RNA folding into a native ribonucleoprotein complex. *Nature Struct. Biol.* **8**, 135-140.
- Treiber, D. K. & Williamson, J. R. (2001). Beyond kinetic traps in RNA folding. *Curr. Opin. Struct. Biol.* **11**, 309-314.

19. Brion, P. & Westhof, E. (1997). Hierarchy and dynamics of RNA folding. *Annu. Rev. Biophys. Biomol. Struct.* **26**, 113-137.
20. Mathews, D. H., Sabina, J., Zuker, M. & Turner, D. H. (1999). Expanded sequence dependence of thermodynamic parameters improves prediction of RNA secondary structure. *J. Mol. Biol.* **288**, 911-940.
21. Walter, N. G., Hampel, K. J., Brown, K. M. & Burke, J. M. (1998). Tertiary structure formation in the hairpin ribozyme monitored by fluorescence resonance energy transfer. *EMBO J.* **17**, 2378-2391.
22. Bassi, G. S., Mollegaard, N. E., Murchie, A. I. & Lilley, D. M. (1999). RNA folding and misfolding of the hammerhead ribozyme. *Biochemistry*, **38**, 3345-3354.
23. Lafontaine, D. A., Norman, D. G. & Lilley, D. M. (2001). Structure, folding and activity of the VS ribozyme: importance of the 2-3-6 helical junction. *EMBO J.* **20**, 1415-1424.
24. Maguire, J. L. & Collins, R. A. (2001). Effects of cobalt hexammine on folding and self-cleavage of the Neurospora VS ribozyme. *J. Mol. Biol.* **309**, 45-56.
25. Been, M. D. & Wickham, G. S. (1997). Self-cleaving ribozymes of hepatitis delta virus RNA. *Eur. J. Biochem.* **247**, 741-753.
26. Ferre-D'Amare, A. R., Zhou, K. & Doudna, J. A. (1998). Crystal structure of a hepatitis delta virus ribozyme. *Nature*, **395**, 567-574.
27. Lai, M. M. (1995). The molecular biology of hepatitis delta virus. *Annu. Rev. Biochem.* **64**, 259-286.
28. Lazinski, D. W. & Taylor, J. M. (1995). Regulation of the hepatitis delta virus ribozymes: to cleave or not to cleave? *RNA*, **1**, 225-233.
29. Karayiannis, P. (1998). Hepatitis D virus. *Rev. Med. Virol.* **8**, 13-24.
30. Reid, C. E. & Lazinski, D. W. (2000). A host-specific function is required for ligation of a wide variety of ribozyme-processed RNAs. *Proc. Natl Acad. Sci. USA*, **97**, 424-429.
31. Robertson, H. D., Manche, L. & Mathews, M. B. (1996). Paradoxical interactions between human delta hepatitis agent RNA and the cellular protein kinase PKR. *J. Virol.* **70**, 5611-5617.
32. Chadalavada, D. M., Knudsen, S. M., Nakano, S. & Bevilacqua, P. C. (2000). A role for upstream RNA structure in facilitating the catalytic fold of the genomic hepatitis delta virus ribozyme. *J. Mol. Biol.* **301**, 349-367.
33. Zuker, M., Mathews, D. H. & Turner, D. H. (1999). Algorithms and thermodynamics for RNA secondary structure prediction: a practical guide. In *RNA Biochemistry and Biotechnology* (Barciszewski, J. & Clark, B. F. C., eds), NATO ASI Series, Kluwer Academic Publishers, Dordrecht.
34. Kumar, P. K., Taira, K. & Nishikawa, S. (1994). Chemical probing studies of variants of the genomic hepatitis delta virus ribozyme by primer extension analysis. *Biochemistry*, **33**, 583-592.
35. Kierzek, R., Burkard, M. E. & Turner, D. H. (1999). Thermodynamics of single mismatches in RNA duplexes. *Biochemistry*, **38**, 14214-14223.
36. Pan, T. & Sosnick, T. R. (1997). Intermediates and kinetic traps in the folding of a large ribozyme revealed by circular dichroism and UV absorbance spectroscopies and catalytic activity. *Nature Struct. Biol.* **4**, 931-938.
37. Shelton, V. M., Sosnick, T. R. & Pan, T. (1999). Applicability of urea in the thermodynamic analysis of secondary and tertiary RNA folding. *Biochemistry*, **38**, 16831-16839.
38. Matysiak, M., Wrzesinski, J. & Ciesiolka, J. (1999). Sequential folding of the genomic ribozyme of the hepatitis delta virus: structural analysis of RNA transcription intermediates. *J. Mol. Biol.* **291**, 283-294.
39. Perrotta, A. T. & Been, M. D. (1991). A pseudoknot-like structure required for efficient self-cleavage of hepatitis delta virus RNA. *Nature*, **350**, 434-436.
40. Perrotta, A. T. & Been, M. D. (1993). Assessment of disparate structural features in three models of the hepatitis delta virus ribozyme. *Nucl. Acids Res.* **21**, 3959-3965.
41. Wadkins, T. S., Perrotta, A. T., Ferre-D'Amare, A. R., Doudna, J. A. & Been, M. D. (1999). A nested double pseudoknot is required for self-cleavage activity of both the genomic and antigenomic hepatitis delta virus ribozymes. *RNA*, **5**, 720-727.
42. Turner, D. H., Sugimoto, N. & Freier, S. M. (1990). Thermodynamics and kinetics of base-pairing and of DNA and RNA self-assembly and helix coil transition. In *Landolt-Börnstein Numerical Data and Functional Relationships in Science and Technology*, vol. 1C, pp. 201-227, Springer, Heidelberg.
43. Luptak, A., Ferre-D'Amare, A. R., Zhou, K., Zilm, K. W. & Doudna, J. A. (2001). Direct pK(a) measurement of the active-site cytosine in a genomic hepatitis delta virus ribozyme. *J. Am. Chem. Soc.* **123**, 8447-8452.
44. Been, M. D., Perrotta, A. T. & Rosenstein, S. P. (1992). Secondary structure of the self-cleaving RNA of hepatitis delta virus: applications to catalytic RNA design. *Biochemistry*, **31**, 11843-11852.
45. Nakano, S., Chadalavada, D. M. & Bevilacqua, P. C. (2000). General acid-base catalysis in the mechanism of a hepatitis delta virus ribozyme. *Science*, **287**, 1493-1497.
46. Perrotta, A. T., Shih, I. & Been, M. D. (1999). Imidazole rescue of a cytosine mutation in a self-cleaving ribozyme. *Science*, **286**, 123-126.
47. Ferre-D'Amare, A. R. & Doudna, J. A. (2000). Crystallization and structure determination of a hepatitis delta virus ribozyme: Use of the RNA-binding protein U1A as a crystallization module. *J. Mol. Biol.* **295**, 541-556.
48. Perrotta, A. T. & Been, M. D. (1990). The self-cleaving domain from the genomic RNA of hepatitis delta virus: sequence requirements and the effects of denaturant. *Nucl. Acids Res.* **18**, 6821-6827.
49. Lee, C. B., Lai, Y.-C., Ping, Y.-H., Huang, Z.-S., Lin, J.-Y. & Wu, H.-N. (1996). The importance of the helix 2 region for the *cis*-cleaving and *trans*-cleaving activities of hepatitis delta virus ribozymes. *Biochemistry*, **35**, 12303-12312.
50. Gluick, T. C. & Draper, D. E. (1994). Thermodynamics of folding a pseudoknotted mRNA fragment. *J. Mol. Biol.* **241**, 246-262.
51. Cate, J. H., Hanna, R. L. & Doudna, J. A. (1997). A magnesium ion core at the heart of a ribozyme domain. *Nature Struct. Biol.* **4**, 553-558.
52. Wu, M. & Tinoco, I., Jr. (1998). RNA folding causes secondary structure rearrangement. *Proc. Natl Acad. Sci. USA*, **95**, 11555-11560.
53. Nakano, S., Proctor, D. J. & Bevilacqua, P. C. (2001). Mechanistic characterization of the HDV genomic ribozyme: assessing the catalytic and structural contributions of divalent metal ions within a multi-

- channel reaction mechanism. *Biochemistry*, **40**, 12022-12038.
54. Nakano, S. & Bevilacqua, P. C. (2001). Proton inventory of the genomic HDV ribozyme in Mg^{2+} -containing solutions. *J. Am. Chem. Soc.* **123**, 11333-11334.
55. Makino, S., Chang, M. F., Shieh, C. K., Kamahora, T., Vannier, D. M., Govindarajan, S. & Lai, M. M. (1987). Molecular cloning and sequencing of a human hepatitis delta (δ) virus RNA. *Nature*, **329**, 343-346.
56. Weeks, K. M. & Cech, T. R. (1996). Assembly of a ribonucleoprotein catalyst by tertiary structure capture. *Science*, **271**, 345-348.
57. Batey, R. T. & Williamson, J. R. (1998). Effects of polyvalent cations on the folding of an rRNA three-way junction and binding of ribosomal protein S15. *RNA*, **4**, 984-997.
58. Gluick, T. C., Gerstner, R. B. & Draper, D. E. (1997). Effects of Mg^{2+} , K^+ , and H^+ on an equilibrium between alternative conformations of an RNA pseudoknot. *J. Mol. Biol.* **270**, 451-463.
59. Perrotta, A. T., Nikiforova, O. & Been, M. D. (1999). A conserved bulged adenosine in a peripheral duplex of the antigenomic HDV self-cleaving RNA reduces kinetic trapping of inactive conformations. *Nucl. Acids Res.* **27**, 795-802.

Edited by J. Doudna

(Received 4 September 2001; received in revised form 15 January 2002; accepted 17 January 2002)